Determination of Yarn Production Characteristics Using Image Processing

Vítor H. Carvalho,[1] Michael S. Belsley,[2] Rosa M. Vasconcelos,[3] Filomena O. Soares[1]

[1] Department of Industrial Electronics, Minho University, Campus de Azurém, 4800-058 Guimarães, Portugal

[2] Department of Physics, Minho University, Campus de Gualtar, 4710-057 Braga, Portugal

[3] Department of Textile Engineering, Minho University, Campus de Azurém, 4800-058 Guimarães, Portugal

Received 20 September 2008; accepted 28 September 2010

ABSTRACT: This article describes a low-cost image acquisition and processing system, which measures several yarn production characteristics, namely, the fibers twist orientation, the folded yarn twist step, the folded yarn twist orientation, and the existence of single (nonfolded yarn) or multiple cables (folded yarn). The imaging hardware consists of a USB web camera coupled to an analog microscope and a monochromatic light source. The acquired images are analyzed using custom designed software based on the IMAQ Vision image program from National Instruments. A full description of the developed image processing tool is presented, together with several experimental results. The results obtained are consistent with information deduced from high-resolution images acquired using an electron microscope. © 2010 Wiley Periodicals, Inc. Int J Imaging Syst Technol, 20, 391–399, 2010; Published online in Wiley Online Library (wileyonlinelibrary.com). DOI 10.1002/ima.20259

Key words: yarn production characteristics; IMAQ Vision; system design

I. INTRODUCTION

Four particularly important production characteristics of commercial yarns are the fiber's twist orientation, the number of cables (folded yarns consisting of more than one cable), the folded yarn twist step, and the folded yarn twist orientation (Neves, 1968; Goswami et al., 1977; Foster, 1982; Castro and Araújo, 1986). The latter two production characteristics mentioned are relevant only in the case of folded yarns. Figure 1 identifies these four production characteristics using as an example an electron microscope image of a 4.2 g/km cotton yarn. Two separate cables are clearly visible and so it is a folded yarn. The folded yarn twist step is 333.4 μm, with a clockwise orientation and a fiber twist orientation that is opposite (anticlockwise) to the folded yarn direction.

Correspondence to: Vítor H. Carvalho; e-mail: vcarvalho@dem.uminho.pt

Grant sponsor: Portuguese Foundation (FCT) scholarship; Grant number: SFRH/BD/24025/2004

In Textile Industry, there is no commercially available equipment or even known prototypes capable of automatically obtaining these yarn production characteristics. Instead, they are obtained manually by unaided visual inspection or by using an analog microscope (Goswami et al., 1977; Castro and Araújo, 1986). However, the results obtained are highly susceptible to errors, especially the measurement of the yarn twist step, considering the high precision required for a reliable measurement. To overcome this limitation, we have developed an automatic yarn characterization system based on image acquisition and subsequent image processing, capable of measuring these four important yarn production characteristics.

II. IMAGE SOURCE HARDWARE

To keep the total system price at an acceptable level, a low-cost analog microscope was coupled to a common web CMOS camera. The microscope provides sufficient amplification and image detail, while there are no special requirements regarding the camera resolution. Figure 2 shows a flowchart of the designed system.

The analog microscope used is the Brolux AI from Bresser (http://www.bresseroptics.co.uk), which has the following main characteristics:

- Two oculars of 5× and 16×;
- Three objectives of 4×, 10×, and 40×;
- A Barlow lens of 2×; and
- Led illumination.

For the images described in this work, the 5× ocular lens was used, together with the 4× objective and the 2× Barlow lens, leading to an overall optical amplification of 40× (5 × 4 × 2). This amplification level was sufficient to obtain reliable results for yarns with a wide range of linear masses. However, if necessary, alternative magnifications can be used within the limits of the available set of lenses.

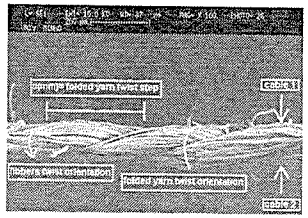

Figure 1. Yarn production characteristics identification.

The USB web camera used is the Deluxe model from Hercules (http://www.hercules.com), which has the following characteristics:

- Photosensitive element: 1/4" CMOS sensor;
- Resolution: 640 × 480 pixels;
- Video mode: VGA; and
- Color format: 24 bit—true color.

The web camera was placed at the exit plane of the microscope ocular, capturing the analog image produced by the microscope. With an optical amplification of 40×, a sensor resolution of 640 × 480 pixels is adequate to correctly evaluate the yarn production characteristics.

To obtain higher contrasts for the yarn geometry relief, the illuminated yarn surface must be as close as possible to a monochromatic light source. As the white led illumination available with the microscope emits a wide range of wavelengths, we decided to use an external yellow light source, which is somewhat closer to an ideal monochromatic light source. Figure 3 illustrates two different images acquired when using the white light source from the microscope and the external yellow light source, respectively.

As these images show, with the yellow light source, the contrast between the yarn zones with higher relief is more accentuated. The regions that correspond to the most accentuated twist areas of yarn areas, which are closer to the light source (as seen in Fig. 1), are more clearly distinguished.

To analyze the acquired images, an image processing application was developed using the IMAQ Vision software from LabVIEW from National Instruments.

III. DEVELOPED SOFTWARE APPLICATION

The developed application consists of three different sections (A, B, and C). For each section described in the following, we demonstrate the influence of the technique used, using two examples of the several different yarns studied during the development of the system. The methodologies used were validated through the common commercial range of 100% cotton linear mass yarns.

Figure 2. Designed system flowchart.

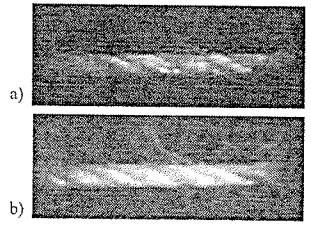

Figure 3. Source images resulting from white (a) and yellow (b) illumination.

A. Main Application Development. The raw images were processed with the following functions from the IMAQ Vision software to arrive at images that allow one to easily determine the production characteristics of a given yarn:

1. Contrast adjust: expressed as a value between 1 and 89. The median value of 45 corresponds to a neutral setting, no contrast alteration, while higher values produce greater contrast. As it was intended to increase the contrast of the relief transition zones, the maximum value (89) was selected (Klinger, 2003; Relf, 2003; IMAQ, 2004).
2. Gamma adjust: this specifies the value considered in Gamma correction. Higher coefficients are associated with weaker intensity corrections. As it was intended to reduce as much as possible the intensity correction, to separate the relief transition zones, the highest value (10) was used (Klinger, 2003; Relf, 2003; IMAQ, 2004).

Figure 5 presents the results obtained on the original image (Fig. 4), after adjusting the contrast and gamma, to their highest values.

As a result of the steps 1 and 2, all pixels with intensities lower than those acquired in the transition zones have been effectively set to 0 intensity.

3. To simplify the binary image conversion process, it is desirable to homogenize the color distributions in the image presented in Figure 5. This can be accomplished using the "Removal of the Luminance Plane over the Hue Saturation Luminance (HSL) Color Space" tool (Klinger, 2003; Relf, 2003; IMAQ, 2004).

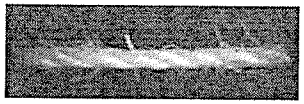

Figure 4. Original image as acquired by the web camera.

Figure 5. The resulting image after setting the contrast to 89 and the gamma adjust to 10. [Color figure can be viewed in the online issue, which is available at wileyonlinelibrary.com.]

Figure 6 presents the resulting image after applying the Removal of the Luminance Plane on the image in Figure 5.

This step converted the three different tonalities presented in Figure 5, namely, red, yellow, and white, to dark gray, light gray, and white, reducing significantly the color intensity spectrum of the original image.

4. Auto Threshold: Intervariance: the threshold function consists of segmenting an image into two regions, namely, a "particle" region and a background region, setting to "1" all the image pixels with a gray level equal to or above a given gray level threshold (threshold interval) and setting to "0" all the other pixels. This process is used to isolate certain areas in an image. To select the threshold interval automatically, the Auto Threshold Interclass Variance tool was used. This method determines an optimal threshold level by maximizing the between-class variation with respect to the threshold. The threshold value is the pixel value (gray level) chosen as the threshold) at which Eq. (1) (variance) is maximized (Klinger, 2003; Relf, 2003; IMAQ, 2004),

$$\sigma_B^2(k) = \frac{\left[\mu_T \omega(k) - \mu(k)\right]^2}{\omega(k)\left[1 - \omega(k)\right]} \quad (1)$$

where, k is the number of gray levels in the image. The numbers $p(i)$ are the occurrence probability of a given gray level i, namely

$$p(i) = \frac{h(i)}{\sum_{i=0}^{k} h(i)}; \quad (2)$$

Here, $h(i)$ represents the total number of pixels with a given gray level value i.

Figure 7 shows the resulting image after applying the Auto Intervariance function to Figure 6. As expected, the application of the binary algorithm has isolated all the pixels with the relevant information (pixels different from black color, in this case).

5. Hole Filling: this function fills the holes within continuous bright parts of the image to homogenize the binary images (Klinger, 2003; Relf, 2003; IMAQ, 2004).

The application of the Hole Filling function to Figure 7 is illustrated in Figure 8; three holes identified in Figure 7 by the white arrows have been filled.

6. Erosion: this function eliminates isolated pixels in the background and erodes the contour of particles according to a defined structuring element. This structuring element is a 2D binary mask, which defines the size and effect of the neighborhood on each pixel, controlling the effect of the binary morphological function on the shape and boundary of a particle. In this case, we considered a 3×3 matrix containing values of 1. For a certain pixel P0, the structuring element is centered on P0. If the coefficient of the structuring element is equal to 1, the marked pixels are referred as Pi (Klinger, 2003; Relf, 2003; IMAQ, 2004):

   a. If the value of one pixel Pi is equal to 0, then P0 is set to 0 otherwise P0 is set to 1.
   b. If the logical AND of Pi is equal to 1, then P0 is set to 1, otherwise P0 is set to 0.

This function eliminates unwanted particles and avoids the possibility of object aggregation. Figure 9 presents the application of the Erosion function described above to the image of Figure 8. As a result, the particles are now well separated. This is especially important for those particles that were particularly close to one another (identified with white arrows in Fig. 8), which could easily been considered as one particle, rather than two. In addition, almost all the other irrelevant information has been also removed.

7. Convex Hull: this function closes particles to allow measurements even when the particle contour is discontinuous. It calculates a convex envelope around each particle, closing it (Klinger, 2003; Relf, 2003; IMAQ, 2004). This function was used to allow use to carry out the necessary particle measurements.

As Figure 10 shows, the application of the Convex Hull function drastically reduces the discontinuity of the particles observed in Figure 9.

8. Small Objects Removal: This step is based on successive applications of the erosion tool followed by dilatation.

Figure 6. Image resulting from the application of the Removal of the Luminance Plane over the HSL to the image of Figure 5.

Figure 7. Image resulting from the application of the Auto Threshold, Intervariance, to the image of Figure 6.

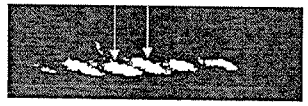

Figure 8. Image resulting from the application of the Hole Filling function to the image in Figure 7.

This results in the elimination of the small particles and smoothing of the larger particle boundaries. Since erosion and dilatation are complementary transformations, for large particles, this operation does not significantly change the area or the shape as the borders removed by the erosion function are restored by the dilatation function (Klinger, 2003; Relf, 2003; IMAQ, 2004).

The result of a single application of this operation is shown in Figure 11. The small particle identified by the white arrow in Figure 10 has been removed in Figure 11, maintaining the other particles essentially unaltered. However, as this algorithm is for general use and, as in some cases, the undesired small particles are slightly larger than the particles eliminated by a single iteration, a double iteration of this operation was used. In this example, the first particle on the right was eliminated (Fig. 12a). However, the loss of this particle is of little consequence as the number of particles remaining is enough to determine the desired parameters.

9. Particle Analysis: This function is used to perform several types of measurements over the particles of a binary image. Specifically in this study, the following parameters were used (Klinger, 2003; Relf, 2003; IMAQ, 2004):

   a. First horizontal pixel: the horizontal coordinate of the first particle pixel.
   b. Determination of orientation: the angle (α) of the line that passes through the particle center of mass corresponding to the lowest moment of inertia [Eq. (3)]. The orientation angle is measured counter clockwise using the horizontal axis as a reference, over a range between 0° and 180° (190° is reported as a 10° angle).

$$\alpha(o) = \frac{1}{2}\arctan\left(\frac{2\,\mu_{xy}}{\mu_{xx} - \mu_{yy}}\right) \quad (3)$$

   where, x and y are, respectively, the horizontal and vertical pixel coordinates of the line corresponding to the lowest moment of inertia.

   c. Area: area of the particle.

Figure 9. Image resulting from the application of the Erosion function to the image of Figure 8.

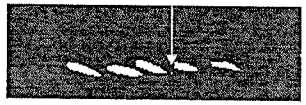

Figure 10. Image resulting from the application of the Convex Hull function to the image of Figure 8.

Considering the parameters obtained with the Particle Analysis function, it was possible to classify the yarn production characteristics, as presented next in Section B.

B. Yarn Production Characteristics Classification. On carrying out the above imaging processing procedures, it is possible to apply the following steps to determine the desired yarn production characteristics:

- Folded yarn twist step, which is the average of the horizontal pixel distance between particles: This parameter is only relevant when the yarn contains more than one cable (folded yarn), i.e., when at least two particles have been identified.
- Folded yarn twist orientation: This parameter is determined by the orientation angle for each particle:
  - If the orientation angle lies between 90° and 180°, then the twist orientation is anticlockwise.
  - If the orientation angle lies between 0° and 90°, then the twist orientation is identified as being in the clockwise direction. Of course, the yarn must have at least two cables (folded yarn) to make it possible to determine the folded yarn twist orientation.
- Number of cables (folded or nonfolded yarn):
  - If only one particle is identified, then the yarn is identified as a single cable (nonfolded yarn).
  - If the number of particles is greater than one, then the yarn is identified as possessing multiple cables (folded yarn).
- Fibers twist orientation: two possible situations may occur:
  - When the yarn is constituted by more than one cable (folded yarn), the fibers twist orientation is opposite to the folded yarn twist orientation. This is a universal situation in Textile Industry, done to avoid untwisting of the fibers over the yarns (Goswami et al., 1977; Castro and Araújo, 1986).

Figure 11. Image resulting from the first application of the Small Objects Removal function to the image of Figure 10.

Figure 12. Image resulting from the second application of the Small Objects Removal function.

- When considering a single cable yarn (nonfolded yarn), a new function is called. The description of this algorithm is presented next in Section C.

C. Application Developed for Classification of the Twist Orientation in Single Cable Yarns. To obtain the fibers twist orientation in nonfolded yarns, the following algorithm was used:

1. Removal of the intensity plane of the hue, saturation, and intensity color encoding scheme: In single cable yarns, a large region of the yarn should have a high-intensity level (Klinger, 2003; Relf, 2003; IMAQ, 2004). With the removal of the intensity plane, the intensity distribution over the yarn becomes more homogeneous.

Figure 13 presents the original yarn image, and Figure 14 shows the result after the removal of the intensity plane, which produces a much more uniform intensity distribution.

2. Convolution—highlight details: A convolution is an algorithm that recalculates the value of a pixel based on its own value and the pixel values of its neighbors weighted by the coefficients of a convolution kernel. The convolution kernel defines how the associated filter alters the pixel values in a grayscale image. It is a 2D structure whose coefficients define how the filtered value at each pixel is computed. Considering several iterative tests, a 7×7 kernel containing 60 in the center and -1 at all the other positions was used (Klinger, 2003; Relf, 2003; IMAQ, 2004). Two iterations were performed to obtain a good definition of the high relief fibers (closer to the light source) which constitute the yarn.

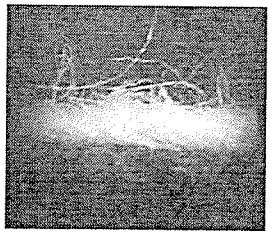

Figure 13. Image used for the development of the twist orientation for a single cable yarn.

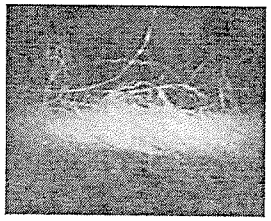

Figure 14. Image resulting from the application of the intensity plane of the HIS color scheme.

Figure 15 presents the result of the convolution after the first iteration. Figure 16 presents the result after the second iteration. The image of Figure 14 is used as the base reference for the image processing techniques applied next.

It was observed that only two iterations are needed to greatly increase the visibility of the exterior yarn fibers.

3. Auto Threshold Moments: The threshold moments method is based on the assumption that the observed image is a blurred version of the theoretical binary original. The blurring that is produced from the acquisition process, caused by electronic noise or a slight imperfection in the optics, is assumed not to alter significantly either the average or the variance of the pixels intensity distribution. This function recalculates a theoretical binary image. The kth moment m of an image is calculated by Eq. (4) (Klinger, 2003; Relf, 2003; IMAQ, 2004).

$$m_k = \frac{1}{n}\sum_{i=0}^{255} i^k h(i) \tag{4}$$

where, n is the total number of pixels in the image.

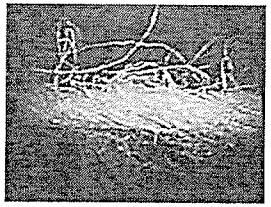

Figure 15. Image resulting from the application of the Convolution function to the image of Figure 14.

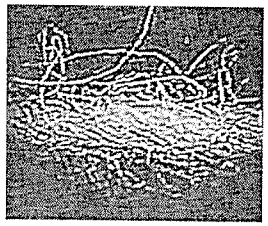

Figure 16. Image resulting from the second application of the Convolution function.

The Auto Threshold Moments were considered to isolate the white details obtained in Figure 16.

Figure 17 presents the results obtained after the application of the Auto Threshold Moments function on the image of Figure 16, showing an excellent isolation of the image details.

4. Small Objects Removal: This option was used to remove all the small particles present in Figure 17 (Klinger, 2003; Relf, 2003; IMAQ, 2004).

Figure 18 presents the results obtained on applying the Small Objects Removal tool to the image of Figure 17.

5. Labeling: This function assigns a different gray level value to each particle in the image. The result is not a binary image but a labeled image which uses a number of gray level values equal to the number of particles in the image, plus the gray level zero assigned to the background area. This function identifies particles using either connectivity-4 or connectivity-8 criteria. The connectivity criteria define the neighborhood a given pixel. For connectivity-4, only adjacent pixels in the horizontal and vertical directions are considered neighbors, for connectivity-8, all adjacent pixels are considered neighbors. For the cases studied, connectivity-4 produced better results (Klinger, 2003; Relf, 2003; IMAQ, 2004). This reduces the influence of the neighborhood pixels and subsequently produces a more differentiated gray level labeling of the particles corresponding to fibers which protrude from the yarn core.

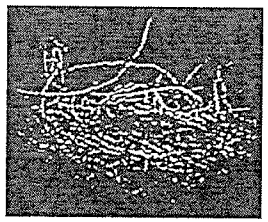

Figure 17. Image resulting from the application of the Auto Threshold Moments function to the image of Figure 16.

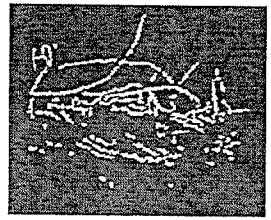

Figure 18. Image resulting from the application of the Small Objects Removal function to the image in Figure 17.

Figure 19 presents the results of the Labeling function used on the image of Figure 18. As observed, the binary image has been separated into several objects, identified by different colors and where the protruding particles are displayed with a lower gray level.

6. Exponential: This function decreases brightness and increases contrast in bright regions of an image, decreasing contrast in dark regions (Klinger, 2003; Relf, 2003; IMAQ, 2004). Here, this step was important to eliminate fibers protruding from the yarn core.

Figure 20 presents the result of applying the exponential function to Figure 19. Besides removing the protruding particles, the

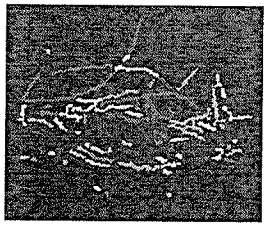

Figure 19. Image resulting from the application of the Labeling function to the image of Figure 18.

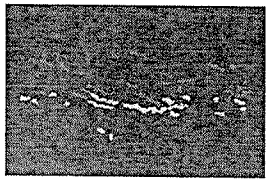

Figure 20. Image resulting from the application of the Exponential function to the image of Figure 19.

labeling color in the remaining particles has changed, due to the alterations in brightness.

7. Convex Hull: As in section A, this function was used to permit the necessary particle measurements (Klinger, 2003; Relf, 2003; IMAQ, 2004).

After the application of the convex hull tool to the image of Figure 20, the image in Figure 21 was obtained. As intended, the level of discontinuity of each particle has been reduced.

8. Particle Filter: The goal of this function is to remove all the particles with reduced areas. Considering multiple case studies, it was concluded that for the optical amplification used, removing all particles with an area inferior to 34 pixels (threshold) allows proper results (Klinger, 2003; Relf, 2003; IMAQ, 2004).

Figure 22 presents the use of the particle area filter in the previous image.

9. Particle Analysis—Orientation: Measuring the orientation angle of each particle enables the determination of the twist orientation (Klinger, 2003; Relf, 2003; IMAQ, 2004). The considered strategy calculates the average orientation of all particles in the image. Then, as in section B:

a. If the average angle orientation lies between 90° and 180°, then the twist orientation is anticlockwise.
b. Conversely, if the orientation angle is within the interval from 0° to 90°, then the twist orientation is clockwise.

Figure 21. Image resulting from the application of the Convex Hull function to the image in Figure 20.

Figure 22. Image resulting from the application of the Particle Area Filter function to the image of Figure 21.

D. Image Calibration. To calibrate the images, we have acquired an image of an object with known dimensions as shown in Figure 23.

In Figure 23, the real world distance between the lines is 1 mm, while in the acquired image, this distance was found to be 73 pixels. This means that a single pixel corresponds to 1/73 mm.

IV. RESULTS

This section presents the results obtained with the developed image processing techniques applied to four different cotton linear mass yarns, namely, 62 g/km (Fig. 13), 55 g/km (Fig. 24), 50 g/km (Fig. 25), and 22 g/km (Fig. 4).

For the 22 g/km yarn, the image processing application obtained the final image presented in Figure 12. The corresponding Particle Analysis data is presented in Table I.

The average distance between particles together with its standard deviation is 29.3 ± 8.3 pixels. Considering the data obtained in Table I, the following yarn production characteristics were determined:

- Fibers twist orientation: clockwise;
- Folded yarn twist orientation: anticlockwise;
- Number of cables: more than one cable (folded yarn); and
- Folded yarn twist step: 0.4 ± 0.1 mm.

Figure 26 shows the final 50 g/km yarn image after image processing while Table II displays the Particle Analysis data obtained.

The distance between the particles is 56.00 pixels. Considering the data obtained in Table II, the following yarn production characteristics were determined:

- Fibers twist orientation: clockwise;
- Folded yarn twist orientation: anticlockwise;
- Number of cables: more than one cable (folded yarn); and
- Folded yarn twist step: 0.77 mm.

For the 55 g/km yarn, the final image obtained after image processing is presented in Figure 27, while the corresponding Particle Analysis data is presented in Table III.

Figure 23. Image used for calibrating the system with real world measurements.

Figure 24. Initial image of the 55 g/km yarn.

Figure 25. Initial image of the 50 g/km yarn.

Table I. Results obtained for the 22 g/km yarn.

Particles	First Horizontal Pixel	Orientation (°)	Area (pixels)
1	52	162.9	128
2	88	168.8	148
3	198	161.6	126
4	140	165.0	83

Figure 26. Image resulting from the developed application in the 50 g/km yarn.

Table II. Results obtained for the 50 g/km yarn.

Particles	First Horizontal Pixel	Orientation (°)	Area (pixels)
1	78	160.0	156
2	134	169.4	276

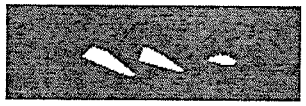

Figure 27. Image resulting from the application developed in the 55 g/km yarn.

Table III. Results obtained for the 55 g/km yarn.

Particles	First Horizontal Pixel	Orientation (°)	Area (pixels)
1	73	154.5	377
2	116	158.0	292
3	181	174.6	120

Figure 28. Image resulting from the application developed in the 62 g/km yarn.

Table IV. Results obtained for the 62 g/km yarn.

Particles	First Horizontal Pixel	Orientation (°)	Area (pixels)
1	132	176.6	8527

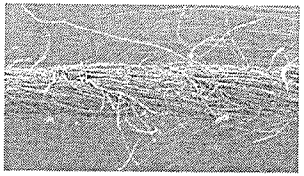

Figure 29. Electron microscope picture of the 50 g/km yarn.

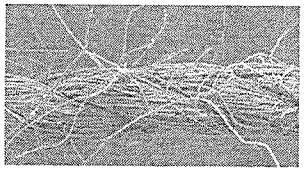

Figure 30. Electron microscope picture of the 55 g/km yarn.

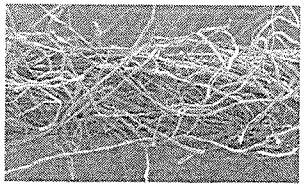

Figure 31. Electron microscope picture of the 62 g/km yarn.

In this case, the distance between particles is 54 ± 15 pixels. Considering the data obtained in Table III, the following yarn production characteristics were determined:

- Fibers twist orientation: clockwise;
- Folded yarn twist orientation: anticlockwise;
- Number of cables: more than one cable (folded yarn); and
- Folded yarn twist step: 0.7 ± 0.2 mm.

For the 62 g/km yarn, the final image obtained after image processing is shown in Figure 28 and the resulting Particle Analysis data is listed in Table IV.

As just one particle was detected, this is a single yarn cable and the function of twist orientation described previously in section C was activated. A particle orientation angle of 136° was obtained (Fig. 22) and the following yarn production characteristics were determined:

- Fibers twist orientation: anticlockwise;
- Folded yarn twist orientation: not available;
- Number of cables: one cable (non folded yarn); and
- Folded yarn twist step: not available.

Afterward, to show that the obtained image processing results are valid and reliable, they were compared with the parameters deduced from detailed electronic microscope pictures (amplification factor of 40×), for yarns of 50, 55, and 62 g/km, represented in Figures 29–31, respectively.

Observing Figures 29 and 30 for 50 g/km and 55 g/km yarns, it is verified that these yarns are formed by more than one cable (folded yarns), with a folded yarn twist orientation, anticlockwise, and a fibers twist orientation in the clockwise direction. Considering Figure 31 (62 g/km), it is verified that this yarn is constituted by a single cable (unfolded yarn), with a fibers twist orientation in anticlockwise direction. Moreover, a folded yarn twist step between 0.74 mm and 0.82 mm has been measured over the image, for the 50 g/km, and between 0.64 mm and 0.78 mm, for the 55 g/km yarn. These results, obtained from the electron microscope images, are in agreement with the results obtained with the developed image processing tool.

V. CONCLUSIONS AND FUTURE WORK

This article presents a low-cost system for determining yarn production characteristics. The system includes, a USB web camera coupled to microscope optics using monochromatic illumination. An appropriate image processing algorithm was developed using the IMAQ Vision software from National Instruments. This custom application performs the analysis of an image source and determines the desired yarn production characteristics, namely, the fibers twist orientation, the folded yarn twist step, the folded yarn twist orientation, and the number of cables (folded or nonfolded yarn). Moreover, the system was validated by comparing the developed application results with electron microscope images.

This work was a part of a PhD project where the main goal was to develop an integrated yarn quality classification system using capacitive and optical sensors for irregularity and hairiness analysis (Carvalho et al., 2006a,b; 2007a,b; 2008). At this point, each of the individual system modules has been developed and integrated together to comprise a complete laboratory prototype. Future work will concentrate on the development of a robust commercially viable solution. Additionally, the possibility of measuring all system parameters using only image acquisition and processing is being taken into consideration as an alternative.

REFERENCES

V. Carvalho, P. Cardoso, M. Belsley, R. Vasconcelos, and F. Soares, Determination of yarn hairiness using optical sensors. EUROSENSORS XX, 17–19 September, Gothenburg, Sweden. 2006a.

V. Carvalho, P. Cardoso, M. Belsley, R. Vasconcelos, and F. Soares, Development of a yarn evenness measurement and hairiness analysis system. IECON06, 7–10 November, Paris, France. 2006b.

V. Carvalho, P. Cardoso, M. Belsley, R. Vasconcelos, and F. Soares, A new automated reference method for yarn hairiness quantification, ISIE 2007, 4–7 June, Vigo, Spain. 2007a.

V. Carvalho, P. Cardoso, M. Belsley, R. Vasconcelos, and F. Soares, Optical yarn hairiness measurement system, IMDT307, 25–27 July, Vienna, Austria. 2007b.

V. Carvalho, P. Cardoso, M. Belsley, R. Vasconcelos, and F. Soares, Yarn hairiness parameterization using a coherent signal processing technique, Sens Actuators A 145 (2008), 217–224.

M. Castro and M. Araújo,Manual de Engenharia Têxtil, Vol. II. Gulbenkian, Lisbon, 1986.

R. Furter, Evenness testing in yarn production. Part I. The Textile Institute and Zellweger Uster AG, Manchester, 1982.

B. Goswami, J. Martindale, and F. Scardino, Textile yarns: Technology, structure and applications, 2nd ed., Wiley, New York, 1977.

IMAQ. IMAQ Vision concepts manual. National Instruments, Austin, 2004.

T. Klinger, Image processing with LabVIEW and IMAQ Vision. Prentice Hall, New Jersey, 2003.

J.S. Neves, A Irregularidade dos Fios Têxteis, sua origem, medição e análise. Oporto, 1968.

C.G. Relf, Image acquisition and processing with LabVIEW, CRC, Boca Raton, 2003.